Mesh-Centered Finite Differences from Nodal Finite Elements

Jean-Pierre Hennart, Edmundo del Valle

INRIA

INSTITUT NATIONAL DE RECHERCHE EN INFORMATIQUE ET EN AUTOMATIQUE

Mesh-Centered Finite Differences from Nodal Finite Elements

Jean-Pierre Hennart and Edmundo del Valle

N° 2979

August 1996

THÈME 4

ISSN 0249-6399

Mesh-Centered Finite Differences from Nodal Finite Elements

Jean-Pierre Hennart*and Edmundo del Valle†

Thème 4 — Simulation et optimisation
de systèmes complexes
Projet Estime

Rapport de recherche n ° 2979 — August 1996 — 44 pages

Abstract: After it is shown that the classical five points mesh-centered finite difference scheme can be derived from a low order nodal finite element scheme by using nonstandard quadrature formulae, higher order block mesh-centered finite difference schemes for second-order elliptic problems are derived from higher order nodal finite elements with nonstandard quadrature formulae as before, combined to a procedure known as "transverse integration". Numerical experiments with uniform and nonuniform meshes and different types of boundary conditions confirm the theoretical predictions, in discrete as well as continuous norms.

Key-words: Nodal methods, mesh-centered finite difference schemes

(Résumé : tsvp)

The first author (JPH) is on sabbatical leave from IIMAS-UNAM, Apdo Postal 20.726, 01000 México D.F. (MEXICO) and also Consultant at the "Comisión Nacional de Seguridad Nuclear y Salvaguardias" (MEXICO)

* Jean-Pierre.Hennart@inria.fr
† Instituto Politécnico Nacional, Escuela Superior de Física y Matemáticas, Unidad Profesional "Adolfo López Mateos", 07738 México D.F. (MEXICO), Edmundo@esfm.ipn.mx

Unité de recherche INRIA Rocquencourt
Domaine de Voluceau, Rocquencourt, BP 105, 78153 LE CHESNAY Cedex (France)
Téléphone : (33 1) 39 63 55 11 – Télécopie : (33 1) 39 63 53 30

Différences Finies Centrées à partir d'Eléments Finis Nodaux

Résumé : Après avoir montré que le schéma en différences finies centré classique à cinq points peut être obtenu à partir d'un élément fini nodal de bas ordre en utilisant des formules de quadrature numériques non standard, on développe des schémas à cinq blocs d'ordre plus élevé avec des quadratures numériques non standard comme plus haut, combinées avec une procédure connue sous le nom d'intégration transversale. Des expériences numériques avec des mailles uniformes ou pas et différents types de conditions à la frontière, confirment les prédictions théoriques en normes continues et discrètes.

Mots-clé : Méthodes nodales, schémas centrés en différences finies

1 Introduction

In this paper, it is shown how point and block mesh-centered finite difference schemes can be derived from nodal finite element schemes, using some nonstandard numerical quadratures elementwise as well as a procedure called *transverse integration* for the block schemes.

Section 2 recalls the classical version of the five points mesh-centered finite difference scheme, which can be viewed as a finite volume scheme with mass conservation property. The basic equation considered here is a standard second order elliptic equation, which actually is the "battle horse" of the multigroup diffusion calculations performed on a routine basis in nuclear engineering. Our choice stems from the fact that nodal methods where first applied to that kind of equation in the late 70s. The presence of a positive absorption or "reaction" term leads to the diagonal dominance of the resulting algebraic equations and explains the success of the standard iteration procedures in production codes.

Section 3 recalls the general family of nodal finite elements developed in Hennart [13], namely RTk, where "nodal finite elements" refers to (nonconforming) finite elements with unknowns which are cell and edge moments, and not point values and/or derivatives as with classical finite elements. After introducing some notation in order to clearly define the spaces and the sets of degrees of freedom to be used, the general family of nodal finite elements mentioned above is recalled in a very compact way. These schemes are then used to approximate the solution of the equation considered. The classical primal variational formulation of the problem is recalled. As only k edge moments are conserved between neighboring cells, the approximations are not continuous, i.e. they correspond to "nonconforming" finite element schemes. Well-known error estimates in the presence of nonconformity as well as numerical quadratures (to be used extensively in Sections 4 and 5) are collected with the appropriate references. Finally, some comments are made about the effects of the presence of "singularities" due to the piecewise constant character of the coefficients: this explains in particular why we limited ourselves to RTk schemes with $k \leq 1$.

It should be pointed out here that our notation for the nodal schemes considered reminds that they are related to the Raviart-Thomas mixed finite elements [25] when a mixed-hybrid formulation is used followed by an exten-

sion à la Arnold-Brezzi [2]. This extension as shown in [2] is what allows to obtain $O(h^{k+2})$ convergences continuously, i.e. in "continuous norms", when the solution is smooth enough. Full details can be found in Hennart and del Valle [19].

Section 4 shows that the classical five points mesh-centered scheme can be derived from a RT0 nodal scheme provided some nonstandard quadrature rules are used to evaluate the elementary mass and stiffness matrices. These rules ensure in particular the mass conservation property, which is the most important feature for mesh centered finite difference schemes, no matter how one derives them. They are different depending on which elementary matrix (mass or stiffness) is evaluated and are compatible with an order of convergence in $O(h^2)$ in L^2 norm. The approach here is based on a primal nonconforming nodal finite element formulation: by a very simple postprocessing operation, a fully piecewise continuous approximation can be recovered which exhibits second order continuously.

Russel and Wheeler [26] have shown that the same classical scheme can be derived from the lowest order Raviart-Thomas mixed method [25] when a carefull combination of tensor product trapezoidal and midpoint quadrature rules is used and obtain first order discrete convergences only, for the scalar as well as for the vector variables, as it could be expected in a mixed formulation.

In Section 5, higher order schemes are considered by extending the previous ideas to the RTk nodal schemes with $k \geq 1$. Actually, that section only deals with the $k = 1$ scheme, as schemes with $k > 1$ are not really justified in the nodal context where the coefficients of the original equation are piecewise constant, that is constant over each cell, but different from one cell to the other, and thus "discontinuous".

In the higher order ($k \geq 1$) cases, quadrature rules compatible with convergence rates of $O(h^{k+2})$ are needed as for the low order case, but moreover a procedure called "transverse integration" must be used. The basic idea consists in proceeding to some transverse averaging of the given equation in all the dimensions minus one, in order to stay with only one–dimensional equations. These one-dimensional equations are coupled by "transverse leakage terms" which arise from that part of the partial differential operator which is integrated exactly. This procedure is given explicitly in Section 5 for the two dimensional case, where it is shown moreover how to use transverse integration and

special quadrature rules compatible with convergence rates of $O(h^3)$ to finally obtain a block mesh-centered finite difference scheme with 4×4 blocks. After a simple postprocessing operation is applied, the resulting approximation is of third order continuously.

By using a generalization of the Russell-Wheeler technique [26], Ewing and Shen [10, 27] obtain a similar block scheme. The numerical quadratures they use are tensor products of Lobatto rules by Gauss ones. Notice that the trapezoidal rule used in [26] is the lowest order Lobatto rule while the midpoint rule is the lowest order Gauss rule. See e.g. Davis and Rabinowitz [9]. The main differences between this paper and the Ewing and Shen's papers are first the fact that they start from a mixed formulation, and not the primal one used here. Moreover their error estimates are only in discrete error norms, while in this paper, $O(h^3)$ is achieved in a continuous way with an extension of the postprocessing operation mentioned above.

In Section 6, a general theorem for any $k \geq 1$ is demonstrated after some interesting numerical quadrature results are given, showing that the procedure given in Section 5 can be extended to any $k \geq 1$. In this paper, we decided to restrict ourselves to the $k \leq 1$ cases in Sections 4 and 5, for reasons explained in Section 3 which have to do with the fact that we are dealing with discontinuous coefficients. For smooth coefficients, it is not excluded to think of higher order methods and the theoretical results of Section 6 show that this is always possible.

Finally, Section 7 is devoted to some numerical experiments with the point and block mesh-centered finite difference schemes derived here from a nodal finite element point of view. They fully corroborate the predictions of Sections 4 and 5 and moreover show superconvergence phenomena for some of the discrete parameters.

2 The mesh-centered finite difference scheme

In this section, we recall the classical version of the five points mesh–centered finite differences scheme.

Let us consider the equation

$$Lu \equiv -\nabla \cdot p\nabla u + qu = f \quad , \quad \forall \mathbf{r} \in \Omega \subset \mathbb{R}^n, \tag{2.1}$$

where u is subject to boundary conditions on $\Gamma = \overline{\Omega} - \Omega$, for instance

$$u = 0 \quad , \quad \forall \mathbf{r} \in \Gamma_1, \tag{2.2}$$

and

$$\frac{\partial u}{\partial n} = 0 \quad , \quad \forall \mathbf{r} \in \Gamma_2, \tag{2.3}$$

with $\Gamma = \Gamma_1 \cup \Gamma_2$ and $\Gamma_1 \cap \Gamma_2 = \phi$. Here and in the following, we shall always assume that the domain Ω is a fairly regular domain, e.g., of the "union of rectangles" type, which can be thus discretized in rectangular elements Ω_e:

$$\Omega \equiv \Omega_h = \bigcup_{e=1}^{E} \Omega_e, \tag{2.4}$$

and where the coefficients p and q are assumed to be piecewise constant, that is p and q are constant over each Ω_e.

In numerical reactor calculations, p and q are in fact quite heterogeneous. The standard procedure consists of a (usually multistage) homogenization whereby they are replaced by equivalent diffusion parameters over fairly large regions called nodes, from whence came the name of nodal methods, which appeared in the nuclear engineering literature in the 1960s. See e.g. Lawrence [21]. In the finite element jargon, "node" is instead a point of an element to which degrees of freedom are attached. To avoid any confusion in the following, we shall consistently use "cell" instead of "node".

Each Ω_e can be viewed as an elementary cell C_{ij} associated to the point (i, j) which is the center of gravity of C_{ij} (See Figure 1 for the notation). In the context of the transverse integration procedure which will be introduced in Section 5, the cell C_{ij} is at the intersection of the i^{th} vertical slice with the j^{th} horizontal one.

The five points mesh–centered finite difference scheme is obtained by looking for an approximation u_h of u satisfying the balance equation

$$\int_{C_{ij}} (Lu_h - f)\, d\mathbf{r} = 0, \tag{2.5}$$

over each elementary cell. Using the divergence theorem, this becomes

$$-\int_{\Gamma_{ij}} p\nabla u_h \cdot \mathbf{n}\, ds + \int_{C_{ij}} (qu_h - f)\, d\mathbf{r} = 0, \tag{2.6}$$

where $\Gamma_{ij} = \overline{C}_{ij} - C_{ij} = \overline{abcda}$ and all boils down to *how* we are going to approximate $p\nabla u_h \cdot \mathbf{n}$ on $\Gamma_{ij} = \overline{abcda}$. On $\overline{ab}$ for instance, we can think of an approximation like

$$p\nabla_{u_h} \cdot \mathbf{n} \simeq p_{\overline{ab}} \frac{u_{i+1,j} - u_{ij}}{R}, \tag{2.7}$$

where $p_{\overline{ab}} \equiv p_{i+1/2,j}$ has to be defined in some way as a function of $p_O \equiv p_{ij}$ and $p_R \equiv p_{i+1,j}$. This can be done by expressing that

$$p_{i+1/2,j} \frac{u_{i+1,j} - u_{ij}}{R} = p_O \frac{u_{i+1/2,j} - u_{ij}}{0.5\Delta x_i} = p_R \frac{u_{i+1,j} - u_{i+1/2,j}}{0.5\Delta x_{i+1}}, \tag{2.8}$$

which allows us to obtain $u_{i+1/2,j}$ and $p_{i+1/2,j}$ as

$$u_{i+1/2,j} = \frac{\frac{p_O u_{ij}}{\Delta x_i} + \frac{p_R u_{i+1/2,j}}{\Delta x_{i+1}}}{\frac{p_O}{\Delta x_i} + \frac{p_R}{\Delta x_{i+1}}} \quad , \tag{2.9}$$

and

$$p_{i+1/2,j} = \frac{\Delta x_i + \Delta x_{i+1}}{\frac{\Delta x_i}{p_O} + \frac{\Delta x_{i+1}}{p_R}}. \tag{2.10}$$

Using equations (2.7), (2.9), and (2.10), we finally get

$$-\int_{\overline{ab}} p\nabla u_h \cdot \mathbf{n}\, ds \simeq \frac{2\Delta y_j}{\frac{\Delta x_i}{p_O}+\frac{\Delta x_{i+1}}{p_R}}(u_{ij}-u_{i+1,j}), \tag{2.11}$$

and

$$\int_{C_{ij}} (qu_{ij}-f)\, d\mathbf{r} \simeq (q_O u_{ij}-f_O)\Delta x_i \Delta y_j, \tag{2.12}$$

we obtain the final expression

$$\begin{aligned} \frac{2\Delta y_j}{\frac{\Delta x_i}{p_O}+\frac{\Delta x_{i+1}}{p_R}}(u_{ij}-u_{i+1,j}) &+ \frac{2\Delta y_j}{\frac{\Delta x_i}{p_O}+\frac{\Delta x_{i-1}}{p_L}}(u_{ij}-u_{i-1,j}) \\ +\frac{2\Delta x_i}{\frac{\Delta y_i}{p_O}+\frac{\Delta y_{j+1}}{p_T}}(u_{ij}-u_{i,j+1}) &+ \frac{2\Delta x_i}{\frac{\Delta y_i}{p_O}+\frac{\Delta y_{j-1}}{p_B}}(u_{ij}-u_{i,j-1}) \\ +q_O u_{ij}\Delta x_i \Delta y_j &= f_O \Delta x_i \Delta y_j, \end{aligned} \tag{2.13}$$

i.e. the classical *five points mesh-centered finite difference formula*, relating a given point to its closest 4 neighbors.

3 The nodal methods RTk

In order to clearly define the spaces S of polynomials and the corresponding sets D of degrees of freedom to be used later, some notation is necessary.

First of all, we define the following elementary spaces of polynomials in two dimensions ($n = 2$), extensions to three dimensions being trivial

$$\mathcal{Q}_{k\ell} \equiv \{x^\alpha y^\beta \quad , \quad 0 \le \alpha \le k \quad , \quad 0 \le \beta \le \ell\}, \tag{3.1}$$

with in particular

$$\mathcal{Q}_k \equiv \mathcal{Q}_{kk}, \tag{3.2}$$

as well as

$$\mathcal{P}_k \equiv \{x^\alpha y^\beta \quad , \quad 0 \leq \alpha + \beta \leq k\}. \tag{3.3}$$

As we mentioned previously, the basic parameters with nodal methods will be cell and (or) edge moments. For practical purposes, these moments will be taken as Legendre moments. Let P_i be the normalized Legendre polynomial over $[-1, +1]$ satisfying

$$P_i(+1) = 1 \quad , \quad P_i(-1) = (-1)^i \quad . \tag{3.4}$$

and

$$\int_{-1}^{+1} P_i(x)P_j(x)\,dx = N_i\delta_{ij} \quad , \tag{3.5}$$

with $N_i = 2/(2i+1)$. Moreover, define $P_{ij}(x,y)$ as $P_i(x)P_j(y)$.

Any particular rectangular cell or element can always be mapped by a diagonal affine transformation onto the reference cell $C \equiv [-1,+1] \times [-1,+1]$. Over C, cell moments of an approximation $u_h(x,y) \in S$ of $u(x,y)$ are defined as follows

$$m_C^{ij}(u_h) = \int_C P_{ij}(x,y)u_h(x,y)\,dxdy/N_i \cdot N_j. \tag{3.6}$$

Moreover, edge moments are given by

$$m_E^i(u_h) = \int_E P_i(s_E)u_h(x_E, y_E)\,ds_E/N_i, \tag{3.7}$$

where E is a generic symbol for the left (L), right (R), bottom (B), and top (T) edges, respectively; x_E or y_E is ± 1, depending on the particular edge considered; and the other coordinate along that edge is s_E.

In Hennart [13], a general family of nodal schemes is introduced which are related to the mixed finite elements of Raviart-Thomas [25] in 2 dimensions, as shown in Hennart and del Valle [19]. After the appearence of the nodal concept in the early 1960s, modern nodal methods were in fact developed in numerical reactor calculations in the late 1970s. These methods are consistent in the sense that they converge to the exact solution of the given equation in the limit of a vanishing mesh. A general reference is the review paper by Lawrence [21]. As we have shown in several papers, these methods are related to nonconforming finite element methods. However these methods are "nonstandard" in several aspects.

First of all, the basic unknowns are not point values or derivatives but instead *cell and edge moments*.

Let us recall here that in the numerical reactor calculation terminology, "node" in principle refers to a fairly large, homogenized region, usually the quarter of an assembly or even a whole assembly in the reactor core. In the present nuclear engineering literature, nodal methods have almost completely replaced the classical finite element, finite difference and finite volume methods which are practically the only ones mentioned in the textbooks on numerical partial differential equations. Most of the Annual and Winter Meetings of the American Nuclear Society (ANS), as well as the Topical Meetings every two years of the Mathematics and Computation Division of the ANS have sessions entirely devoted to nodal methods, not only for diffusion but also for transport problems, in static or time-dependent situations. Their standard derivation is based on the conservation of physical properties such as mass balance and continuity (at least in the mean) of the scalar variable (u) and of the corresponding flux ($\mathbf{v} = -p\nabla u$). Such conservation properties are related to the use in a classical nonconforming approach of quite specific or *adhoc quadrature rules*, which have been analyzed in particular in Hennart and del Valle [13, 19] and will be recalled in the next two sections.

To this second nonstandard feature, we must add a third one which is pervasive in the nuclear engineering literature, namely the use of *transverse integration* procedures by which a multidimensional problem is replaced by

a set of coupled one-dimensional problems. Transverse integration has been analyzed in [19] and will be briefly recalled in Section 5.

Last but not least, there is a whole class of nodal methods which relie on the use of *quasipolynomial functions*, including in particular exponential basis functions. These functions arise quite naturally in the context of transverse integration procedures. The numerical analysis of these so-called *analytical* nodal methods can be found in Hennart [14]. Higher order analytical methods have been presented for instance in Ougouag and Rajic [24] and in Altiparmakov and Tomašević [1]. In this work, we shall restrict ourselves to purely polynomial methods.

These few remarks should make clear that nodal methods cannot be viewed simply as variants of well-known and understood methods. Their analysis requires completely specific mathematical techniques, where nonconformity, adhoc numerical quadratures and quasipolynomial functions may be present altogether. The evident success of nodal methods in nuclear engineering calculations shows that there is clearly an audience for this work. There is moreover a lot of applications in other fields like in general fluid flow in porous media (aquifers, oil reservoirs, etc.), and in particular diffusion and transport of contaminants underground or in the atmosphere, for which nodal methods are especially well suited: over meshes which are at least topologically of the union of rectangles type, the coefficients in the leading equations are not well-known and are therefore generally replaced by piecewise constants over coarse meshes. For these problems, the industrial simulators classically relie on finite differences or volumes. More recent research works put the emphasis on the use of mixed or mixed hybrid finite element methods, which have a clear nodal flavor as we shall see later.

Let us first recall the general RTk basis functions in 2D as derived in [13]. RT clearly stands for Raviart-Thomas, while k is an index related to the order of convergence of the corresponding scheme: for a given k, the order of convergence in L^2 norm is $(k+2)$ *provided the solution is smooth enough.* RT0 is thus in principle a second order scheme while RT1 is of third order. The set D of parameters is given by $D \equiv \{m_E^i, i = 0, \cdots, k; m_C^{ij}, i, j = 0, \cdots, k\}$ and the corresponding space S is $\mathcal{Q}_{k+2,k} + \mathcal{Q}_{k,k+2}$ with $card(D) = dim(S) = (k+1)(k+5)$. The nodal basis functions are

$$
\begin{aligned}
u_C^{ij}(x,y) &= P_{ij}(x,y) - P_{k+m(i),j}(x,y) - P_{i,k+m(j)}(x,y), \quad i,j = 0,\ldots,k,\\
u_L^i(x,y) &= (-1)^{k+1}\frac{1}{2}(P_{k+1,i}(x,y) - P_{k+2,i}(x,y)), \quad i = 0,\ldots,k,\\
u_R^i(x,y) &= +\frac{1}{2}(P_{k+1,i}(x,y) + P_{k+2,i}(x,y)), \quad i = 0,\ldots,k,\\
u_B^i(x,y) &= u_L^i(y,x), \quad i = 0,\ldots,k,\\
u_T^i(x,y) &= u_R^i(y,x), \quad i = 0,\ldots,k,
\end{aligned} \tag{3.8}
$$

where $m(i)$ (resp. $m(j)$) $= 1$ or 2 and is such that $k + m(i)$ (resp. $k + m(j)$) has the same parity as i (resp. j) . The particular cases $k = 0$ and $k = 1$ have will be considered in the next two sections.

The general determination of the space S to be used given a set D of degrees of freedom, and then of the corresponding basis functions, has been treated in detail in Hennart, Jaffré, and Roberts [16]. We should also mention that there are other mixed finite element families, for instance in Brezzi, Douglas, and Marini [4] or in Brezzi et al. [5], from which other nodal finite element methods can be derived: in particular, nodal finite elements with less parameters than RT1 but the same order can be developed as shown in Hennart et al. [17].

The classical primal variational formulation of our problem (2.1) with the boundary conditions (2.2) and (2.3) consists of finding $u \in U = H^1_{0,\Gamma_1}(\Omega)$ such that

$$
a(u,v) = f(v), \quad \forall v \in U, \tag{3.9}
$$

where $a(u,v) \equiv \int_\Omega (p\nabla u \cdot \nabla v + quv)\, d\mathbf{r}$, $f(v) \equiv \int_\Omega fv\, d\mathbf{r}$ with $H^1_{0,\Gamma_1}(\Omega) = \{v | v \in H^1(\Omega), v|_{\Gamma_1} = 0\}$, H^1 being the standard Sobolev space.

A conforming approximation of u is obtained by looking for $u_h \in U_h \subset H^1_{0,\Gamma_1}(\Omega)$ with $dim(U_h) < \infty$ such that

$$
a(u_h, v_h) = f(v_h), \quad \forall v_h \in U_h. \tag{3.10}
$$

Because the schemes mentioned previously provide only the continuity of one or two moments of u_h at cell boundaries, u_h itself is not continuous and

$$U_h \not\subset H^1_{0,\Gamma_1}(\Omega), \tag{3.11}$$

so that u_h is a *nonconforming approximation* of u. Equation (3.10) should be modified accordingly, and $a(u_h, v_h)$ should be replaced by $a_h(u_h, v_h)$, where

$$a_h(u_h, v_h) = \sum_{e=1}^{E} \int_{\Omega_e} p \nabla u_h \cdot \nabla v_h \, d\mathbf{r} + \int_{\Omega} q u_h v_h \, d\mathbf{r}. \tag{3.12}$$

The nonconforming u_h will converge to u if and only if some "patch test" is passed. See e.g. Strang and Fix [28].

At this point, it is interesting to collect well known error estimates when nonconformity is present and also when the matrix elements appearing in Eq. (3.12) are not calculated exactly but rather approximated by numerical quadrature, as used in the following sections. A general reference about error estimates is Chap. 4 of Ciarlet [7] or his article in [8]. As we have seen previously, $\Omega \equiv \Omega_h$, so that the only variational crimes in the sense of Strang and Fix [28] commited here are related to the nonconformity and to the use of quadrature rules.

With conforming elements and exact integration, all depends on the approximation properties of the space S, which in turn depends on the greatest $l \in \mathbb{N}_*$, where $\mathbb{N}_*$ is the set of (positive) natural numbers, such that $\mathcal{P}_l \subset S$. Knowing that l, it is possible to predict the behavior of the error $(u - u_h)$ in the H^1 norm, namely, of $O(h^l)$ if u is smooth enough. The H^1 norm is the natural norm for a second order elliptic problem. To get an L^2 estimate, standard Aubin-Nitsche arguments should be applied. See for instance Nitsche [23] and Lesaint [20]. The result is that in the conforming case with exact quadratures, the error in the L^2 norm is of $O(h^{l+1})$ assuming that u is smooth enough. Let us point out that similar results can be proved for the analytical nodal schemes, as shown in [14].

In the nonconforming case, as with nodal finite elements, an additional error term is introduced. With the degrees of freedom chosen here, that error term depends on the number m of moments which are preserved between adjacent cells. In L^2 norm, it is of $O(h^{m+1})$. For a demonstration, see Appendix C of [16].

As we shall see in the following sections, the mass conservation property depends in part on the use of an adhoc numerical quadrature in order to lump the mass matrices involving the q term in (2.1). If moreover, we want to obtain algebraically efficient schemes of the finite difference type, numerical quadrature is also needed at the stiffness matrices level, which depend on the p term in (2.1). The arguments are again quite classical: the quadrature schemes considered must have enough quadrature points to conserve the coercivity of the final bilinear form $a_h^*(u_h, v_h)$ where the superscript refers to the fact that in $a_h(u_h, v_h)$, the integrals are not evaluated exactly but approximately with numerical quadrature rules. These ones, which can be different for different terms, must be sufficiently accurate if we do not want to alter the precision expected with a given scheme. In general, quadrature schemes that are exact for $\mathcal{Q}_{2n+1}$ are compatible with error in the norm L^2 of $O(h^{n+2})$. This is true for the rectangular elements used in this paper: all the technical results are demonstrated in Chap. 4 of [7] in the triangular case, the rectangular case being left for the exercises of that chapter.

All these classical results can be collected in

Theorem 1 *Assuming that the solution u has all the regularity required, one has*

$$\| u - u_h \|_0 \propto h^{\lambda+1}, \tag{3.13}$$

where $\| \cdot \|_0$ is the standard L^2 norm, while $\lambda = min\{l, m, n+1\}$ where l is the greatest positive integer such that $\mathcal{P}_l \subset S$, m is the number of edge moments preserved between adjacent cells, and n is an index related to the accuracy of the quadrature rules used, exact for $\mathcal{Q}_{2n+1}$.

For the RTk family of schemes, the approximation properties of S are given by

$$\mathcal{P}_{k+2-\delta_{k0}} \subset S, \quad \forall k \in \mathbb{N}, \tag{3.14}$$

so that for the first two schemes, l jumps from 1 to 3 (and not 2). For the same two schemes, m and $n+1$ are equal to 1 and 2 respectively, so that λ takes the same values.

In typical nodal situations, where the coefficients in (2.1) are piecewise constant, singularities occur at the corners between different materials and at the boundary re-entrant corners and prevent the solution from being very smooth. As shown by Babuška and Kellogg [3], the *asymptotic* behavior of the error in norm L^2 is of $O(h^{2\alpha})$ where α is a real number between 0 and 1, and which depends on the contrast between the p values of the different materials at a given corner or on the internal angle (between π and 2π) at a boundary re-entrant corner. If we assume that at an internal corner, $p = p_i$ in the different quadrants, with p_1 different from $p_2 = p_3 = p_4$, α depends on the ratio p_1/p_2 and is comprised between 1 when $p_1 = p_2$ (that is in the absence of singularity) and $2/3$ when the ratio tends to 0 or ∞. This limiting case corresponds to a re-entrant corner of $3\pi/2$ which is the only possible case when Ω is of the union of rectangles type. See e.g. Hennart and Mund [18]. As shown theoretically in [3], the solution has however a smooth part, for which (3.13) is presumably valid *far from asymptotic*. This would be the case for a typical nodal situation. Provided the difference between 2α and $k+2$ is not too big, or equivalently provided k is not > 1, (3.13) will be approximately satisfied. This has been demonstrated experimentally by the extensive numerical tests performed in [18]. The RT0 scheme is practically a low-order finite difference scheme as shown in the next section and in Hennart [15]. On the other hand for $k > 1$, the singularities will take over and make Eq. (3.13) impossible in practice. This is the basic motivation for considering here schemes *up to third order but no more* for nodal calculations, where ideally coarse meshes only are considered with piecewise constant coefficients.

Before going to the details of the various schemes considered in the next sections, let us introduce the elementary mass, x stiffness and y stiffness matrices of order N for the RTk scheme as

$$\begin{aligned} M &= (m_{ij}), \\ K_x &= (k_{x,ij}), \end{aligned}$$

and

$$K_y = (k_{y,ij}). \tag{3.15}$$

With $(u, v) = \int_C u(\mathbf{r})v(\mathbf{r})\, d\mathbf{r}$, we have

$$
\begin{aligned}
m_{ij} &= (u_i, u_j), \quad i,j = 1, \ldots, N, \\
k_{x,ij} &= (u_{ix}, u_{jx}), \quad i,j = 1, \ldots, N,
\end{aligned}
$$

and

$$
k_{y,ij} = (u_{iy}, u_{jy}), \quad i,j = 1, \ldots, N. \tag{3.16}
$$

Assume now that the vector $\mathbf{u} = [u_1, \ldots, u_N]^T$ of basis functions is partitioned following

$$
\mathbf{u}^T = [\mathbf{u}_H, \mathbf{u}_C, \mathbf{u}_V]
$$

where

$$
\begin{aligned}
\mathbf{u}_H^T &= [u_L^0, u_R^0, \ldots, u_L^k, u_R^k], \\
\mathbf{u}_C^T &= [u_C^{00}, u_C^{10}, \ldots, u_C^{kk}], \\
\mathbf{u}_V^T &= [u_B^0, u_T^0, \ldots, u_B^k, u_T^k].
\end{aligned} \tag{3.17}
$$

As M, K_x and K_y (which are symmetrical matrices) are partitioned accordingly, we have for instance

$$
M = \begin{pmatrix} M_{HH} & M_{HC} & M_{HV} \\ M_{CH} & M_{CC} & M_{CV} \\ M_{VH} & M_{VC} & M_{VV} \end{pmatrix}. \tag{3.18}
$$

If these matrix elements are evaluated exactly, it is easy to realize that

$$
M_{HV} = K_{x,HV} = K_{y,HV} = 0, \tag{3.19}
$$

so that the coupling between the H (for horizontal) and the V (for vertical) components is only via the cell parameters. By symmetry, Eq. (3.19) is also valid for the transposed matrices (with VH instead of HV as subscript).

4 The five points mesh-centered finite differences from the RT0 nodal finite element

In the standard five–point mesh centered finite difference scheme, the basic unknowns are the approximations of the solution at the centers of gravity of the cells. With Gauss quadrature arguments, these are in fact good approximations of the cell mean values and we might think of developing a five–point scheme from the RT0 scheme where the unknowns would be the mean values of $u_h(x,y)$ over a given cell and its four closest neighbors.

With $k = 0$, the elementary mass matrix corresponding to the q and f terms is a 5 by 5 one with only 8 zero elements (M_{HV} and M_{VH}), namely

$$M^e = \frac{\Delta x \Delta y}{4} \begin{pmatrix} \frac{8}{15} & -\frac{2}{15} & -\frac{2}{5} & 0 & 0 \\ -\frac{2}{15} & \frac{8}{15} & -\frac{2}{5} & 0 & 0 \\ -\frac{2}{5} & -\frac{2}{5} & \frac{28}{5} & -\frac{2}{5} & -\frac{2}{5} \\ 0 & 0 & -\frac{2}{5} & \frac{8}{15} & -\frac{2}{15} \\ 0 & 0 & -\frac{2}{5} & -\frac{2}{15} & \frac{8}{15} \end{pmatrix}, \tag{4.1}$$

To recover a finite difference scheme of the mesh centered type, we must first lump this mass matrix since in 2.13 the contribution of qu only comes from $u_{ij} = u_C^{00}$. It was shown in [13] that this can be done (in fact for any k) by what we called a "nonstandard Radau quadrature" scheme.

For the sake of completeness, we shall recall briefly here how it works in the $k = 0$ case and refer the reader to [13] for the $k > 0$ cases and in particular the $k = 1$ case of Section 5. First of all notice that the zeros of u_L^0 (resp. u_R^0) are $(-\frac{1}{3}, +1)$ (resp. $(-1, +\frac{1}{3})$), i.e. the right (resp. left) Radau quadrature points in the simplest case. When we evaluate the elementary mass matrix over the cell C, each time an edge basis function appears, the Radau quadrature scheme using the opposite Radau points should be used so that the corresponding matrix element vanishes. The elementary mass matrix then reduces to only one non-zero element, namely $(u_C^{00}, u_C^{00}) = \int_C (u_C^{00})^2 \, dxdy$, which if evaluated exactly would give 5.6 – and not the correct value of $4 = meas(C)$. If one restores the asymmetry inherent to the Radau rules by using the relationship

$$P_{00}(x,y) = \sum_E u_E^0(x,y) + u_C^{00}(x,y), \tag{4.2}$$

we finally get

$$(u_C^{00}, u_C^{00}) = (P_{00}, P_{00}) = 4.0, \tag{4.3}$$

as it should be, the terms containing the different u_E^0's being again eliminated by Radau quadrature.
In summary,

$$M^e = \frac{\Delta x \Delta y}{4} \begin{pmatrix} 0 & 0 & 0 & 0 & 0 \\ 0 & 0 & 0 & 0 & 0 \\ 0 & 0 & 4 & 0 & 0 \\ 0 & 0 & 0 & 0 & 0 \\ 0 & 0 & 0 & 0 & 0 \end{pmatrix}, \tag{4.4}$$

with a scaling factor $\frac{\Delta x \Delta y}{4}$ due to the fact that Ω_e is used instead of C. This leads us in (2.13) to the correct q_O term in the left hand side. If $f(x,y)$ is replaced by its average value f_O, the correct right hand side will also show up.

The two point Radau rule in $1D$ is exact for quadratic polynomials. Any of its four possible tensor product versions LB, LT, RB, or RT is thus exact for the members of $\mathcal{Q}_2$ and if they are used to evaluate the elementary stiffness matrix in the x or y direction, the exact result will be produced, for instance

$$K_x^e = \frac{\Delta y}{\Delta x} \begin{pmatrix} 4 & 2 & -6 & 0 & 0 \\ 2 & 4 & -6 & 0 & 0 \\ -6 & -6 & 12 & 0 & 0 \\ 0 & 0 & 0 & 0 & 0 \\ 0 & 0 & 0 & 0 & 0 \end{pmatrix}. \tag{4.5}$$

With the Radau rule in x and y, the exact stiffness matrices couple the left and right or bottom and top edge moments and as a consequence, we

don't come up with mesh-centered like finite difference equations. To achieve this goal, we must use different quadrature schemes to evaluate the x and y stiffness matrices in order to eliminate the undesirable couplings, for instance those involving the opposite vertical left and right components for K_x and the ones between the cell moments and the vertical (bottom and top) edge moments. This means in this case that the blocks $K_{x,CV}$ and $K_{x,VC}$, as well as the elements $K_{x,LR}$ and $K_{x,RL}$ must be cancelled out.

It turns out that in the $k = 0$ case considered in this section $u^0_{Bx} = u^0_{Tx} = 0$ and the CV and VC couplings mentioned above are automatically nonexistent. What finally remains to be done is to eliminate the LR or RL couplings in K_x. To summarize, when we are in the cell C_{ij}, we eliminate at the stiffness level the RL coupling and we do the same for the LR coupling in the next cell to the right $C_{i+1,j}$. Since the coupling CV or VC are automatically non existent, the right edge moment in C_{ij} will only be coupled with the cell moments of C_{ij} and $C_{i+1,j}$. It can thus be eliminated in terms of these cell moments and by repeating the operation over each edge, we'll finally come up with a relationship between the cell moments of C_{ij} and its four neighbors.

We have for instance

$$(u^0_{Rx}, u^0_{Lx}) \propto \int_L dy \cdot \int_B (P_1'(x)^2 - P_2'(x)^2)\, dx, \tag{4.6}$$

so that a quadrature rule in the horizontal direction would do the job if it uses as quadrature points the zeros of $P_1'(x) \pm P_2'(x)$. If x_i is a zero of $P_1' + P_2'$, $(-x_i)$ is by parity considerations a zero of $P_1' - P_2'$. Here as $P_1' + P_2' = P_0 + 3P_1 = 1 + 3x$, we shall have

$$x_1 = -\frac{1}{3}, \quad x_2 = +\frac{1}{3}, \tag{4.7}$$

the corresponding quadrature rule (exact for linear polynomials) being

$$\int_{-1}^{+1} f(x)dx \simeq f(-\frac{1}{3}) + f(+\frac{1}{3}), \tag{4.8}$$

a well–known quadrature of the (open) Newton–Cotes type. Under these quadrature schemes combining Radau (or indeed *exact*) quadrature in the vertical direction and open Newton–Cotes in the horizontal direction, the elementary x stiffness matrix becomes

$$K_x^e = \frac{\Delta y}{\Delta x}\begin{pmatrix} 2 & 0 & -2 & 0 & 0 \\ 0 & 2 & -2 & 0 & 0 \\ -2 & -2 & 4 & 0 & 0 \\ 0 & 0 & 0 & 0 & 0 \\ 0 & 0 & 0 & 0 & 0 \end{pmatrix}. \tag{4.9}$$

It remains to prove that these stiffness matrices lead to the correct p terms in the first two lines of (2.13). The equation for $m_R^0 \equiv u_{i+\frac{1}{2},j}$ comes from the assembly of the elementary K_x matrices of cells (i,j) and $(i+1,j)$. The corresponding elementary mass matrices do not intervene since by Radau quadrature there is no mass associated to the edge parameters. Because of the automatic cancellation in either cell of all couplings with u_{Bx}^0 and u_{Tx}^0, these terms being zero (by exact or equivalently Radau quadrature), and of the couplings of $u_{i+\frac{1}{2},j}$ with $u_{i-\frac{1}{2},j}$ (resp. $u_{i+\frac{3}{2},j}$) in cell (i,j) (resp. $(i+1,j)$) (by Newton Cotes quadrature), the final equation is a relationship between $u_{ij}, u_{i+\frac{1}{2},j}$, and $u_{i+1,j}$ namely

$$p_O\frac{\Delta y_j}{\Delta x_i}(2u_{i+1/2,j} - 2u_{i,j}) + p_R\frac{\Delta y_j}{\Delta x_{i+1}}(2u_{i+1/2,j} - 2u_{i+1,j}) = 0, \tag{4.10}$$

which allows us to eliminate $u_{i+\frac{1}{2},j}$ in terms of u_{ij} and $u_{i+1,j}$. The result is identical to (2.8).

The equation for $m_C^{00} \equiv u_{ij}$ induced by the elementary mass and stiffness on cell (i,j) reads

$$\begin{aligned} p_O\frac{\Delta y_j}{\Delta x_i}(-2u_{i-1/2,j} - 2u_{i+1/2,j} + 4u_{ij}) \quad &+ \quad p_O\frac{\Delta x_i}{\Delta y_j}(-2u_{i,j-1/2} - 2u_{i,j+1/2} + 4u_{ij}) \\ +q_O\Delta x_i\Delta y_j u_{ij} \quad &= \quad f_O\Delta x_i\Delta y_j, \end{aligned} \tag{4.11}$$

which can be transformed into an expression relating u_{ij} to its four closest neighbors $u_{i\pm1,j}$ and $u_{i,j\pm1}$ using (2.8) and similar expressions for the top, left, and bottom edges. It is a simple matter to check that the resulting expression is indeed identical to (2.13).

Once $u_{ij} \equiv m_C^{00}$ has been obtained for each cell C_{ij} by solving the corresponding system of algebraic equations, it is trivial to restore the edge averages by using expressions like (4.10), giving $m_R^0 \equiv u_{i+1/2,j}$ for cell ij. After that postprocessing operation, each cell will be equipped with a full set of cell and edge averages, which will allow us to build up a cellwise continuous interpolation of the approximation $u_h(x,y)$ to $u(x,y)$, using the expressions (3.8) for the cell basis functions. This will permit us in Section 7 to evaluate the error on a fine mesh and to come up with the numerical equivalent of a continuous L^2 error estimate, which by Theorem 1 should be in $O(h^2)$ if u has all the regularity required. Notice that this error is for the solution alone as our approach is through a primal formulation. This on the other hand leads to continuous error estimates, as predicted by the classical theory developed for instance in [7, 8].

Several authors, like Manteuffel and White [22], Forsyth and Sammon [12], and Weiser and Wheeler [29], have shown, by using different methods from the ones used in this paper, that convergence for the classical mesh-centered finite difference or volume method is also of $O(h^2)$. The main difference however is that those papers only show *discrete* convergence orders and not *continuous* ones as here . [22, 12] strictly work in a finite difference or finite volume context, where the idea of a piecewise continuous approximation of the solution is not present. Weiser and Wheeler [29] use a finite element approach, which by the way provides more insight in the treatment of rough coefficients and general boundary conditions. They use a mixed finite element method with approximate integration formulae as in [26], and only prove *discrete* L^2-norm error estimates. Extension to continuous L^2-norms of discrete L^2-norms results obtained in [10, 27] is a direct application of Ewing, Shen, and Wang [11], where a superconvergence property along Gauss lines is taken into account to proceed to this extension.

A few words should still be said about the boundary conditions, which have been assumed throughout to be homogeneous: if they are homogeneous Dirichlet on some edge of cell C_{ij}, it suffices to take the corresponding $u_{i\pm1/2,j}$

or $u_{i,j\pm 1/2}$ equal to zero. In the case of homogeneous Neumann conditions, for instance on the right edge of cell C_{ij}, p_R in equation (4.10) is zero and the boundary condition leads to $u_{i+1/2,j} = u_{ij}$. In general, we shall have $u_{i\pm 1/2,j}$ or $u_{i,j\pm 1/2} = u_{ij}$.

Before we leave this section, we should mention an important result, namely that the scheme derived here satisfies the cell balance equation as well as the current continuity condition. In the case when only Radau quadratures are used, this was proved in [13] for the general case of RTk. Here the fact that we are using a combination of Radau and open Newton Cotes quadrature, depending on the elementary matrix we are evaluating, forces us to modify that demonstration, which is the particular case $k = 0$ of the general Theorem 3 given in Section 6.

5 A five blocks finite difference scheme from the RT1 nodal finite element

In view of what has been done in the previous section, it seems reasonable to look at the next RT scheme, the RT1 one, and to try to develop a five blocks mesh-centered finite difference scheme of higher order (actually 3) where the basic unknowns would be the four cell moments of $u_h(x, y)$ over a given cell and its four closest neighbors.

As in the preceding section, we must first lump the mass matrix. This is done as in Section 4 by a "nonstandard Radau quadrature" scheme as shown in Hennart [13]. This time a three points Radau quadrature is used, these points being the zeros of u_R^0, u_R^1 or u_L^0, u_L^1. We shall not give many details since the procedure has been illustrated in the preceding section and fully described in [13]. Let it suffice to say that the final lumped elementary mass matrix is given by

$$M^e = \frac{\Delta x \Delta y}{4} diag\{0, 0, 0, 0, 4, \frac{4}{3}, \frac{4}{3}, \frac{4}{9}, 0, 0, 0, 0\}. \tag{5.1}$$

This matrix of order 12 is diagonal and only has 4 nonzero elements, while the exact one is not diagonal and has 32 nonzero elements.

The three point Radau rule in $1D$ is exact for quartic polynomials. Any of the four possible tensor product versions (LB, LT, RB or RT) is thus exact for $\mathcal{Q}_4$ polynomials. Here however $(u_{hx})^2$ will have components in $\mathcal{Q}_{42} + \mathcal{Q}_{06}$ and any 3×3 Radau rule will not integrate exactly $(u_{hx})^2$ (and $(u_{hy})^2$).

To come up with a five-block mesh centered finite difference scheme, we must first use different quadrature schemes to eliminate the undesirable couplings. In K_x for instance, we have to eliminate the couplings between the opposite vertical left and right components, and also between the vertical components and the horizontal ones (bottom and top) which are, as we have seen, coupled through the cell moments. This means that the blocks $K_{x,CV}$, $K_{x,VC}$, as well as $K_{x,LR}$ and $K_{x,RL}$ must be cancelled out. In the x direction, the right components of cell C_{ij} will thus only be coupled with the cell components of cells C_{ij} and $C_{i+1,j}$. It will then be possible to eliminate them in terms of the cell components of these two cells and by repeating that operation with the three remaining neighbors $C_{i,j+1}$, $C_{i-1,j}$, and $C_{i,j-1}$, we will end up with an algebraic relationship between the four cell moments of the given cell and the corresponding four cell moments of its four neighbors.

As we have

$$(u^i_{Rx}, u^j_{Lx}) \propto \int_{-1}^{+1} P_i(y) P_j(y)\, dy \int_{-1}^{+1} (P_2'(x)^2 - P_3'(x)^2)\, dx, \quad i, j = 0, 1, \tag{5.2}$$

a quadrature rule in the horizontal direction would be adequate if it uses as quadrature points the zeros of $P_2'(x) \pm P_3'(x)$. If x_i is a zero of $P_2' + P_3'$, $(-x_i)$ is by parity considerations a zero of $P_2' - P_3'$. The weights are then chosen in order to produce a quadrature rule exact for polynomials up to third degree. The resulting scheme is

$$\int_{-1}^{+1} f(x)\, dx = w_a[f(-a) + f(a)] + w_b[f(-b) + f(+b)], \tag{5.3}$$

with

$$a = (-1 + \sqrt{6})/5 \quad ; \quad b = (1 + \sqrt{6})/5, \tag{5.4}$$

and

$$w_a = (3\sqrt{6} - 2)/6\sqrt{6} \quad ; \quad w_b = (3\sqrt{6} + 2)/6\sqrt{6}. \tag{5.5}$$

As we have seen previously u_{hx} has components in $\mathcal{Q}_{03}$. To eliminate its components outside of $\mathcal{Q}_{21}$, we need another ingredient which has been described at length in Hennart and del Valle [19], namely the *transverse integration* procedure. For the sake of completeness, we shall recall it briefly. The basic idea consists in proceeding to some transverse averaging of the given equation in all the dimensions minus one, in order to stay with only one–dimensional equations. These one-dimensional equations are coupled by *transverse leakage terms* which arise from that part of the partial differential operator which is integrated exactly. To illustrate the procedure in two dimensions, let us assume that the domain Ω has been divided in I vertical and J horizontal slices. Each particular cell C_{ij} of size $\Delta x_i \times \Delta y_j$ is at the intersection of the i^{th} vertical slice and of the j^{th} horizontal slice. The original equation (2.1) is then successively multiplied by $p_{j\ell}(y)$, $\ell = 0, 1$, and integrated in y between y_{Bj} and y_{Tj}, $j = 1, \ldots, J$. Here $p_{j\ell}(y)$ is the Legendre polynomial $P_\ell(y)$ scaled to the interval $[y_{Bj}, y_{Tj}]$, namely

$$p_{j\ell}(y) = P_\ell(2(y - (y_{Bj} + y_{Tj})/2)/(y_{Tj} - y_{Bj})), \tag{5.6}$$

If we call y_j the midpoint of this interval, we shall have in particular

$$p_{j0} = 1 \quad \text{and} \quad p_{j1}(y) = \frac{2(y - y_j)}{\Delta y_j}. \tag{5.7}$$

The same operation is similarly performed in the other direction. The result is a set of $2(I + J)$ one-dimensional equations of the generic form

$$-(pu_x)_x + qu = f. \tag{5.8}$$

After transverse integration in the y direction, for instance, $u(x)$ is a transverse moment of order 0 or 1 of $u(x, y)$, namely

$$u(x) \rightarrow u^{y\ell,j}(x) = \int_{y_{Bj}}^{y_{Tj}} p_{j\ell}(y)u(x,y)\,dy / \int_{y_{Bj}}^{y_{Tj}} p_{j\ell}^2(y)\,dy, \tag{5.9}$$

and (5.8) gives rise to a set of equations

$$-(pu_x^{y\ell,j}(x))_x + qu^{y\ell,j}(x) = f^{y\ell,j}(x) + \ell^{y\ell,j}(x), \quad \ell = 0,1; \quad j = 1,\ldots,J, \tag{5.10}$$

where $\ell^{y\ell,j}(x)$ is a *transverse leakage* defined by

$$\ell^{y\ell,j}(x) = \int_{y_{Bj}}^{y_{Tj}} p_{j\ell}(y)(pu(x,y))_y\,dy / \int_{y_{Bj}}^{y_{Tj}} p_{j\ell}^2(y)\,dy. \tag{5.11}$$

The normalization term in (5.9) and (5.11) is equivalent to $\Delta y_j N_\ell/2$ and for $\ell = 0$, for instance, (5.11) becomes

$$\ell^{y0,j}(x) = [pu_y(x,y_{Tj}) - pu_y(x,y_{Bj})]/\Delta y_j, \tag{5.12}$$

which can be interpreted physically as a transverse leakage in the y direction from the cell considered. The generic equation (5.8) is then discretized in the usual finite element way and an approximation u_h of u is looked for. u_{hx} has components in P_{02} and P_{03} and it is easy to realize that they are filtered by taking the transverse moments of order 0 and 1 in y. These components which are eliminated are incidentally outside of the Raviart-Thomas spaces [25] for the components of the vector variable $\nabla u_h = (u_{hx}, u_{hy})$ and in Hennart and del Valle [19] the transverse integration procedure is indeed interpreted in terms of a projection of the gradient of u_h onto these Raviart-Thomas spaces. For more details, the readers are referred to [19] and to the next section.

As the result of using the special quadrature (5.3) and (or) the transverse integration, K_x^e (which by the way retains its symmetry) reduces to

$$K_{x,HH}^e = diag\{6,6,2,2\}, \tag{5.13}$$

$$K^e_{x,CH} = K^{eT}_{x,HC} = \begin{pmatrix} -6 & -6 & 0 & 0 \\ 4 & -4 & 0 & 0 \\ 0 & 0 & -2 & -2 \\ 0 & 0 & \frac{4}{3} & -\frac{4}{3} \end{pmatrix}, \tag{5.14}$$

$$K^e_{x,CC} = diag\{12, 8, 4, \frac{8}{3}\}, \tag{5.15}$$

and

$$K^e_{x,VH} = K^{eT}_{x,HV} = K^e_{x,VC} = K^{eT}_{x,CV} = K^e_{x,VV} = 0. \tag{5.16}$$

K^e_y can be derived in a similar way.

Let us consider for instance K^e_x and partition its lower triangular part as follows

$$K^e_x = \frac{\Delta y}{\Delta x} \begin{pmatrix} a & & & & & & & & & & & \\ a & a & & & & & & & & & & \\ a & a & a & & & & & & & & & \\ a & a & a & a & & & & & & & & \\ h & h & g & g & b & & & & & & & \\ i & i & g & g & c & b & & & & & & \\ g & g & h & h & c & c & b & & & & & \\ g & g & i & i & c & c & c & b & & & & \\ f & f & f & f & d & d & d & d & d & & & \\ f & f & f & f & d & d & d & d & d & d & & \\ f & f & f & f & e & e & e & e & e & e & e & \\ f & f & f & f & e & e & e & e & e & e & e & e \end{pmatrix}. \tag{5.17}$$

We shall denote the submatrix corresponding to a lowercase a to i by the corresponding capital letters. For instance

$$A = \frac{\Delta y}{\Delta x} \begin{pmatrix} a & & & & & & & & & & & \\ a & a & & & & & & & & & & \\ a & a & a & & & & & & & & & \\ a & a & a & a & & & & & & & & \\ 0 & 0 & 0 & 0 & 0 & & & & & & & \\ 0 & 0 & 0 & 0 & 0 & 0 & & & & & & \\ 0 & 0 & 0 & 0 & 0 & 0 & 0 & & & & & \\ 0 & 0 & 0 & 0 & 0 & 0 & 0 & 0 & & & & \\ 0 & 0 & 0 & 0 & 0 & 0 & 0 & 0 & 0 & & & \\ 0 & 0 & 0 & 0 & 0 & 0 & 0 & 0 & 0 & 0 & & \\ 0 & 0 & 0 & 0 & 0 & 0 & 0 & 0 & 0 & 0 & 0 & \\ 0 & 0 & 0 & 0 & 0 & 0 & 0 & 0 & 0 & 0 & 0 & 0 \end{pmatrix}, \tag{5.18}$$

and

$$K_x^e = A + B + \ldots + I. \tag{5.19}$$

Let us first recall that the ordering of the different parameters is given by

$$\mathbf{u} = [u_L^0, u_R^0, u_L^1, u_R^1, u_C^{00}, u_C^{10}, u_C^{01}, u_C^{11}, u_B^0, u_T^0, u_B^1, u_T^1]. \tag{5.20}$$

Matrix A is diagonalized thanks to the special quadrature used and is not affected by the transverse integration in the y direction. This actually decouples the contributions of the vertical faces. The matrices C, D, F and G are naturally zero by orthogonality or by the fact that one of the functions is zero in the matrix element. The nonzero elements of matrix E are cancelled by the transverse integration in the y direction. The elements of matrix B and I are modified by the combined effect of the special quadrature and of the transverse integration. Finally the entries of matrix H are not affected by the special quadrature which is exact for cubic functions and the transverse integration does not modify them.

The equations for $m_C^{k\ell} \equiv u_{ij}^{k\ell}$, $k, \ell = 0, 1$ induced by the elementary mass and stiffness on cell (i, j) read

$$
\begin{aligned}
& p_{ij}\frac{\Delta y_j}{\Delta x_i}(-6u^0_{i-1/2,j} - 6u^0_{i+1/2,j} + 12u^{00}_{ij}) \\
+ \quad & p_{ij}\frac{\Delta x_i}{\Delta y_j}(-6u^0_{i,j-1/2} - 6u^0_{i,j+1/2} + 12u^{00}_{ij}) \\
+ \quad & q_{ij}\Delta x_i \Delta y_j u^{00}_{ij} = \Delta x_i \Delta y_j S^{00}_{ij}, \qquad (5.21)
\end{aligned}
$$

$$
\begin{aligned}
& p_{ij}\frac{\Delta y_j}{\Delta x_i}(4u^0_{i-1/2,j} - 4u^0_{i+1/2,j} + 8u^{10}_{ij}) \\
+ \quad & p_{ij}\frac{\Delta x_i}{\Delta y_j}(-2u^0_{i,j-1/2} - 2u^0_{i,j+1/2} + 4u^{10}_{ij}) \\
+ \quad & \frac{1}{3}q_{ij}\Delta x_i \Delta y_j u^{10}_{ij} = \frac{1}{3}\Delta x_i \Delta y_j S^{10}_{ij}, \qquad (5.22)
\end{aligned}
$$

$$
\begin{aligned}
& p_{ij}\frac{\Delta y_j}{\Delta x_i}(-2u^1_{i-1/2,j} - 2u^1_{i+1/2,j} + 4u^{01}_{ij}) \\
+ \quad & p_{ij}\frac{\Delta x_i}{\Delta y_j}(4u^0_{i,j-1/2} - 4u^0_{i,j+1/2} + 8u^{01}_{ij}) \\
+ \quad & \frac{1}{3}q_{ij}\Delta x_i \Delta y_j u^{01}_{ij} = \frac{1}{3}\Delta x_i \Delta y_j S^{01}_{ij}, \qquad (5.23)
\end{aligned}
$$

and

$$
\begin{aligned}
& p_{ij}\frac{\Delta y_j}{\Delta x_i}(\frac{4}{3}u^1_{i-1/2,j} - \frac{4}{3}u^1_{i+1/2,j} + \frac{8}{3}u^{11}_{ij}) \\
+ \quad & p_{ij}\frac{\Delta x_i}{\Delta y_j}(\frac{4}{3}u^1_{i,j-1/2} - \frac{4}{3}u^1_{i,j+1/2} + \frac{8}{3}u^{11}_{ij}) \\
+ \quad & \frac{1}{9}q_{ij}\Delta x_i \Delta y_j u^{11}_{ij} = \frac{1}{9}\Delta x_i \Delta y_j S^{11}_{ij}. \qquad (5.24)
\end{aligned}
$$

For each edge, for instance the vertical edge separating cells (i, j) and $(i+1, j)$, these are two equations for the corresponding edge moments $u^0_{i+\frac{1}{2},j}$ and $u^1_{i+\frac{1}{2},j}$, namely

$$
\begin{aligned}
& p_{ij}\frac{\Delta y_j}{\Delta x_i}(6u^0_{i+1/2,j} - 6u^{00}_{ij} - 4u^{10}_{ij}) \\
+ \quad & p_{i+1,j}\frac{\Delta y_j}{\Delta x_{i+1}}(6u^0_{i+1/2,j} - 6u^{00}_{i+1,j} + 4u^{10}_{i+1,j}) = 0,
\end{aligned} \tag{5.25}
$$

and

$$
\begin{aligned}
& p_{ij}\frac{\Delta y_j}{\Delta x_i}(2u^1_{i+1/2,j} - 2u^{01}_{ij} - \frac{4}{3}u^{11}_{ij}) \\
+ \quad & p_{i+1,j}\frac{\Delta y_j}{\Delta x_{i+1}}(2u^1_{i+1/2,j} - 2u^{01}_{i+1,j} + \frac{4}{3}u^{11}_{i+1,j}) = 0.
\end{aligned} \tag{5.26}
$$

The first one allows us to express $u^0_{i+\frac{1}{2},j}$ in terms of u^{00}_{ij}, u^{10}_{ij}, $u^{00}_{i+1,j}$, and $u^{10}_{i+1,j}$, getting

$$
u^0_{i+1/2,j} = \frac{\frac{p_{ij}}{\Delta x_i}u^{00}_{ij} + \frac{p_{i+1,j}}{\Delta x_{i+1}}u^{00}_{i+1,j}}{\frac{p_{ij}}{\Delta x_i} + \frac{p_{i+1,j}}{\Delta x_{i+1}}} + \frac{2}{3}\frac{\frac{p_{ij}}{\Delta x_i}u^{10}_{ij} - \frac{p_{i+1,j}}{\Delta x_{i+1}}u^{10}_{i+1,j}}{\frac{p_{ij}}{\Delta x_i} + \frac{p_{i+1,j}}{\Delta x_{i+1}}}, \tag{5.27}
$$

while the second one gives us $u^1_{i+\frac{1}{2},j}$ in terms of $u^{01}_{ij}, u^{11}_{ij}, u^{01}_{i+1,j}$, and $u^{11}_{i+1,j}$, namely

$$
u^1_{i+1/2,j} = \frac{\frac{p_{ij}}{\Delta x_i}u^{01}_{ij} + \frac{p_{i+1,j}}{\Delta x_{i+1}}u^{01}_{i+1,j}}{\frac{p_{ij}}{\Delta x_i} + \frac{p_{i+1,j}}{\Delta x_{i+1}}} + \frac{2}{3}\frac{\frac{p_{ij}}{\Delta x_i}u^{11}_{ij} - \frac{p_{i+1,j}}{\Delta x_{i+1}}u^{11}_{i+1,j}}{\frac{p_{ij}}{\Delta x_i} + \frac{p_{i+1,j}}{\Delta x_{i+1}}}. \tag{5.28}
$$

If we substitute these two expressions for each edge in the four equations (5.24), (5.22), (5.23), and (5.24), the final result is a five 4×4 blocks finite difference scheme relating the four cell moments of the central cell (i, j) to the four corresponding cell moments of the four neighboring cells. The expressions (5.25) and (5.26) for each edge allow us to evaluate a posteriori the edge moments of zeroth and first order. All the edge and cell information can be used to evaluate in a postprocessing operation a $2D$ interpolant using the basis functions given in (3.8).

As all the numerical quadratures used are exact for $\mathcal{Q}_3$ polynomials, the scheme obtained is expected to retain the third order of the exact RT1 scheme, as the numerical experiments of the next section will show.

A few words should now be said about how to implement the boundary conditions, assumed again to be homogeneous. If they are of the Dirichlet type on the right edge of cell (i,j) for instance, it suffices to take $u^j_{i+1/2}=0$, $j=0$ and 1. For boundary conditions of the Neumann type on the right edge again, this becomes

$$u^0_{i+1/2,j} = u^{00}_{ij} + \frac{2}{3}u^{10}_{ij}, \tag{5.29}$$

$$u^1_{i+1/2,j} = u^{01}_{ij} + \frac{2}{3}u^{11}_{ij}, \tag{5.30}$$

which comes from equations (5.25) and (5.26) with no contribution from cell $(i+1,j)$. Similar expressions would be used for the three other edges.

When we only have a combination of Radau quadrature in the horizontal and vertical directions, we showed in [13] that for any RTk scheme those quadratures rules ensured mass balances (weighted with respect to $\mathcal{Q}_k$) over a given cell and current continuity conditions (weighted with respect to $\mathcal{P}_k$) through every edge. Here as in the case $k=0$, the stiffness matrices are evaluated with a combination of Radau rules in one direction and of a nonstandard open rule in the other direction. When $k>0$ and in particular when $k=1$ as in this section, we must moreover take into account the transverse integration procedure. A general theorem valid for any $k\geq 0$, and in particular for the case $k=1$ of this section will be given and demonstrated in the next section.

6 Higher order block schemes

In this section, we shall show that the procedure given in detail in Section 5 can in fact be extended to any $k\geq 1$. We shall first prove that a generalized nonstandard open quadrature exists and is well defined for any k. Using some general properties of the transverse integration procedure, we shall then prove

a general theorem, which is applicable in particular to the $k = 1$ case of the previous section. Finally, we shall collect results given here or in previous papers that show some interesting relationships between different methods primal or not, with or without transverse integration and with different quadrature rules.

For any k, there exist Radau rules in 1D with $k+2$ quadrature points which are exact for $\mathcal{P}_{2k+2}$. For the mass matrices, any tensor product of $k+2$ Radau formulae is exact for $\mathcal{Q}_{2k+2}$. For the stiffness matrices, such a rule would be used in one direction, for instance the vertical one, and a generalization of the nonstandard open quadrature given by (5.3), (5.4), and (5.5) would be used in the remaining direction, here the horizontal one. To eliminate the couplings between opposite unknowns in that direction, we must first remember that

$$(u^i_{Lx}, u^j_{Rx}) \propto \int_L P_i(y)P_j(y)\,dy \cdot \int_B (P\prime_{k+1}(x)^2 - P\prime_{k+2}(x)^2)\,dx, \tag{6.1}$$

so that we need as quadrature points the zeros of $P\prime_{k+1}(x) \pm P\prime_{k+2}(x)$, the cancelation due to a δ_{ij} factor being incidental. Considerations of parity show that it is sufficient to look for the zeros of $P\prime_{k+1} + P\prime_{k+2}$, the zero of $P\prime_{k+1} - P\prime_{k+2}$ having the same absolute value but the opposite sign. Since

$$P\prime_{k+1} = (2k+1)P_k + (2k-3)P_{k-2} + (2k-7)P_{k-4} + \dots, \tag{6.2}$$

and

$$P\prime_{k+2} = (2k+3)P_{k+1} + (2k-1)P_{k-1} + (2k-5)P_{k-3} + \dots, \tag{6.3}$$

we shall have

$$P\prime_{k+1} + P\prime_{k+2} = \sum_{\ell=0}^{k+1}(2\ell+1)P_\ell. \tag{6.4}$$

A generalized nonstandard open quadrature rule exists for any k as a consequence of the following

Theorem 2 *$P\prime_{k+1} + P\prime_{k+2}$ has $(k+1)$ real distinct zeros in $(-1,+1)$, which are in fact the $(k+1)$ right Radau quadrature points (excluding +1).*

Proof. The interior right Radau quadrature points are the $(k+1)$ zeros of $\frac{P_{k+2}-P_{k+1}}{x-1}$, which are known to be real and distinct in $(-1,+1)$ [9]. It is therefore sufficient to show that $(x-1)\{P\prime_{k+1} + P\prime_{k+2}\}$ is proportional to $P_{k+2} - P_{k+1}$. Using (6.4) and the recurrence relationship between Legendre polynomials, namely

$$(\ell+1)P_{\ell+1} = (2\ell+1)xP_\ell - \ell P_{\ell-1}, \tag{6.5}$$

we get

$$(x-1)(P\prime_{k+1} + P\prime_{k+2}) = \sum_{\ell=0}^{k+1}(\ell+1)P_{\ell+1} + \sum_{\ell=1}^{k+1}\ell P_{\ell-1} - \sum_{\ell=0}^{k+1}(2\ell+1)P_\ell, \tag{6.6}$$

where the first and third terms in the lefthand side give contributions to P_{k+2} and P_{k+1}, which combined are proportional to $P_{k+2} - P_{k+1}$ as expected. It is then a simple matter to show that the remaining terms from P_0 to P_k cancel out. Consequently, the $(k+1)$ interior right Radau quadrature points are also the zeros of $P\prime_{k+1} + P\prime_{k+2}$. ■

Since the zeros of $P\prime_{k+1} - P\prime_{k+2}$ are symmetrical in $(-1,+1)$ with respect to the zeros of $P\prime_{k+1} + P\prime_{k+2}$, a generalized nonstandard open quadrature rule exists for any k. This quadrature rule, which we shall call symmetrical Radau rule, has $2(k+1)$ integration points in $(-1,+1)$ and is exact for $\mathcal{P}_{2k+1}$ in $1D$. Combined with a Radau rule with $k+2$ quadrature points in the other direction, one gets schemes exact for $\mathcal{Q}_{2k+1,2k+2}$ or $\mathcal{Q}_{2k+2,2k+1}$ which all contain $\mathcal{Q}_{2k+1}$, so that n in Theorem 1 is identical to k. The schemes obtained are thus compatible with errors in the norm L^2 of $O(h^{k+2})$.

With $S \equiv \mathcal{Q}_{k+2,k} + \mathcal{Q}_{k,k+2}$, it is easy to realize that

$$\nabla u_h \in (\mathcal{Q}_{k+1,k} + \mathcal{Q}_{k-1,k+2}) \times (\mathcal{Q}_{k+2,k-1} + \mathcal{Q}_{k,k+1}), \quad \forall u_h \in S, \quad k > 0, \tag{6.7}$$

or in the particular case $k = 0$

$$\nabla u_h \in \mathcal{Q}_{10} \times \mathcal{Q}_{01}, \quad \forall u_h \in S. \tag{6.8}$$

The Raviart-Thomas [25] space of nonnegative index k is $\mathcal{Q}_{k+1,k} \times \mathcal{Q}_{k,k+1}$. Consequently, *except for* $k = 0, \nabla u_h$ is not in the corresponding Raviart-Thomas space. In [19], we have shown that the transverse integration used for $k \geq 1$ actually projects the gradient of u_h onto the Raviart-Thomas space of index k.

Similarly, we have

$$\Delta u_h \in \mathcal{Q}_k + \mathcal{Q}_{k-2,k+2} + \mathcal{Q}_{k+2,k-2}, \quad \forall u_h \in S, \quad k > 1, \tag{6.9}$$

or when $k \leq 1$

$$\Delta u_h \in \mathcal{Q}_k, \quad \forall u_h \in S, \tag{6.10}$$

this last result becoming true for any k provided the transverse integration is used.

With these auxiliary results, it is possible to prove a general theorem, namely

Theorem 3 *When any tensor product Radau rule is applied to the mass terms while a combination of the Radau rule in one direction and of the symmetrical Radau rule in the other direction is applied to the stiffness terms, and when moreover transverse integration is used when $k \geq 1$, the resulting five blocks mesh-centered finite difference schemes generalize the scheme given in the preceding section by equations (5.21), (5.22), (5.23), and (5.24). In general, these schemes have blocks of order $(k+1)$ and they satisfy the following weighted cell balance equations over each cell*

$$\int_C P_{ij}(\mathbf{r})(-\nabla \cdot p \nabla u_h + q u_h - f)\, d\mathbf{r} = 0, \quad i, j = 0, \ldots, k, \tag{6.11}$$

as well as the following weighted current continuity conditions through the edges

$$\int_E P_i(s_E)[p\nabla u_h|_{C_1} - p\nabla u_h|_{C_2}] \cdot \mathbf{1}_n \, ds_E = 0, \quad i = 0, \ldots, k. \tag{6.12}$$

As shown above in Section 3, we want to find $u_h \in U_h$ such that

$$a_h^*(u_h, v_h) = f^*(v_h), \quad \forall v_h \in U_h. \tag{6.13}$$

a. Let us take as v_h one of the cell basis functions $u_C^{ij}, i, j = 0, \ldots, k$ associated to a cell C. Since that function is nonzero only on C, the equation (6.13) becomes (before quadrature is used)

$$\int_C (p\nabla u_h \cdot \nabla u_C^{ij} + q u_h u_C^{ij} - f u_C^{ij}) \, d\mathbf{r} = 0, \quad i, j = 0, \ldots, k, \tag{6.14}$$

or equivalently

$$\begin{aligned} & \int_{\partial C} u_C^{ij} (p\nabla u_h \cdot \mathbf{1}_n) ds \\ + & \int_C u_C^{ij} \{-\nabla \cdot p\nabla u_h + q u_h - f\} \, d\mathbf{r} = 0, \quad i, j = 0, \ldots, k. \end{aligned} \tag{6.15}$$

Let us first show that the boundary term $\int_{\partial C}$ _____ is zero. On the boundary ∂C, u_C^{ij} reduces to P_{k+1} or to P_{k+2} along the edge considered as it is easily seen from (3.8). Because of the transverse integration which projects ∇u_h onto the Raviart-Thomas space of index k, $p\nabla u_h \cdot \mathbf{1}_n \in \mathcal{P}_k$ on any edge and by orthogonality the boundary term is zero. Let us now treat the cell terms. Using the fact demonstrated in [13] that

$$\begin{aligned} P_{ij}(x, y) = u_C^{ij}(x, y) & + (-1)^i u_L^j(x, y) + u_R^j(x, y) \\ & + (-1)^j u_B^i(x, y) + u_T^i(x, y), \end{aligned} \tag{6.16}$$

it is easy to rewrite $u_h \in U_h$ as $m_C^{00} + \sum_E m_E^{0*} u_E^0$ with $m_E^{0*} = m_E^0 - m_C^{00}$. As the stiffness and mass terms are treated with different quadratures, they must be considered separately. In the mass terms, all the edge contributions to u_C^{ij} are cancelled by the Radau quadrature in x and y, so that u_C^{ij} can be replaced by P_{ij}. On the other hand, for the stiffness terms, only two of the edge contributions are eliminated by Radau quadrature (say the top and bottom ones) so that u_C^{ij} can be replaced by $P_{ij} - (-1)^i u_L^j - u_R^j$ which finally reduces to P_{ij} as u_L^j and u_R^j are orthogonal to $-\nabla \cdot p \nabla u_h$ which belongs to $\mathcal{Q}_k$ by transverse integration. (6.15) reduces thus to the weighted cell balance equation (6.11).

b. Let us now take as v_h the boundary basis function reducing to u_R^i on C_1 and to u_L^i with $i = 0, \ldots, k$ on C_2, C_1 and C_2 being two neighboring cells in the horizontal direction with $\Gamma_{12} = \bar{C}_1 \cap \bar{C}_2$. In that case, (6.13) becomes

$$\begin{aligned} & \int_{C_1} (p \nabla u_h \cdot \nabla u_R^i + q u_h u_R^i - f u_R^0)\, d\mathbf{r} \\ + & \int_{C_2} (p \nabla u_h \cdot \nabla u_L^i + q u_h u_L^i - f u_L^0)\, d\mathbf{r} = 0, \end{aligned} \tag{6.17}$$

which after Radau quadrature for the mass terms and integration by parts leads to

$$\begin{aligned} - & \int_{C_1} \nabla \cdot p \nabla u_h u_R^i \, d\mathbf{r} - \int_{C_2} \nabla \cdot p \nabla u_h u_L^i \, d\mathbf{r} \\ + & \int_{\partial C_1} u_R^i p \nabla u_h \cdot \mathbf{1}_{n_1} \, ds + \int_{\partial C_2} u_L^i p \nabla u_h \cdot \mathbf{1}_{n_2} \, ds = 0. \end{aligned} \tag{6.18}$$

The first two terms are zero by orthogonality, because $\nabla \cdot p \nabla u_h$ belongs to $\mathcal{Q}_k$ due to the transverse integration and is thus orthogonal to any edge function given in (3.8). Since u^i is zero (u_R^i on the left edge of C_1, u_L^i on the right edge of C_2) or by orthogonality on the bottom and top edges with a polynomial of degree k, namely $p \nabla u_h \cdot \mathbf{1}_n$ because of the transverse integration, (6.18) reduces to

$$\int_{\Gamma_{12}} P_i(y)[p\nabla u_h|_{C_1} - p\nabla u_h|_{C_2}] \cdot \mathbf{1}_n \, dy = 0, \quad i = 0, \ldots, k, \tag{6.19}$$

which is the weighted current continuity condition on Γ_{12}. ■

Before leaving this section, we want to put together results obtained earlier or in this paper which show interesting connections between different methods. In [13], we derived the general family of nodal schemes RTk and introduced the concept of *mathematical nodal methods* (MNM) when these nonconforming nodal elements are used without any attempt of satisfying mass balance and flux continuity. General error estimates for these nonconforming methods with exact quadrature have been proved in Appendix C of [16]. In [13] again, we showed that the physical nodal methods (PNM) derived from these MNMs imply the use the Radau rules in all the directions, which in turn is equivalent to the (weighted) balance and flux continuity conditions given by Eqs. (6.11) and (6.12). In [19], a mathematical interpretation of this procedure in terms of L^2 projections has also been developed.

In the same paper, it is also been shown that the Radau procedure for the mass terms only, combined *if* $k > 0$ with the transverse integration, yields a primal nonconforming nodal approximation u_h which is equivalent to a post-processed Raviart-Thomas mixed-hybrid approximation $\tilde{u}_h$. This approximation is deduced from a standard Raviart-Thomas dual mixed approximation, where the normal flux continuity conditions are hybridized, that is relaxed by the introduction of Lagrange multipliers on the edges. These Lagrange multipliers turn out to be edge moments of the scalar variable: in a postprocessing operation developed by Arnold and Brezzi [2], this edge information is combined with the cell information in $\mathcal{Q}_k$ to produce $\tilde{u}_h$ in the same space S as u_h. For details, the readers are referred to [19] where it is proved that the transverse integration is in fact equivalent to a projection of $\nabla u_h \in S$ onto the Raviart-Thomas space $\mathcal{Q}_{k+1,k} \times \mathcal{Q}_{k,k+1}$. As a result, the Radau rule would give the exact stiffness and is only needed for the mass.

Finally, the block schemes developed in this paper use a combination of standard and symmetrical Radau rules to finally come up with schemes which are of the finite difference type and therefore more attractive from an algebraic

point of view. Notice that here again the transverse integration is needed when $k > 0$. As for the preceding schemes (except the MNMs), they satisfy (weighted) balance and flux continuity conditions, which imply that they are very close to postprocessed mixed-hybrid approximations.

7 Numerical experiments

In this section, we exhibit some numerical results obtained with two computer codes, namely MCk0 and MCk1, which implement the methods of index 0 and 1 of Sections 4 and 5. These computer codes were used to solve a test problem chosen have a smooth analytical solution. This allows us to numerically check the convergence rates predicted by the theory. The equation considered was

$$-\Delta u + u = f \quad \text{on} \quad \Omega \in [-1, +1] \times [-1, +1], \tag{6.1}$$

with homogeneous Dirichlet boundary conditions on Γ.

The exact solution for the test problem is as follows

$$u(x, y) = (1 - x^4)(1 - y^4), \tag{6.2}$$

from which $f(x, y)$ is easily derived.

We first solve this test problem over the whole domain Ω with Dirichlet boundary conditions (see Figure 2.a) and then over the reduced domain $\Omega_r = [0, +1] \times [0, +1]$ which corresponds to the first quadrant of Ω but with Neumann boundary conditions at $x = 0$ ($y \in [0, +1]$) and also at $y = 0$ ($x \in [0, +1]$), keeping the Dirichlet boundary conditions at $x = 1$ ($y \in [0, +1]$) and $y = 1$ ($x \in [0, +1]$) (see Figure 2.b).

Besides, we considered uniform and also non–uniform meshes. The uniform meshes were generated as usual and the non–uniform meshes by first splitting the domains Ω and Ω_r as shown in Figures 3.a and 3.b. Each cell of these figures was then spatially discretized by using uniform meshes as indicated in the tables given in this section. Following this procedure, the spatial discretization of the domains shown in Figures 2 (resp. Figures 3) will lead to a uniform (resp. non–uniform) mesh.

For the sake of simplicity, we shall refer to the different cases mentioned above as cases A1, A2, A3 and A4 corresponding to Figures 2.a, 2.b, 3.a, and 3.b respectively.

Thus for each computer code, we have four cases to be considered. In each one of the tables, we give errors ϵ in L^2 norm and calculate the numerical exponent α of $\epsilon \propto h^\alpha$ by comparing two successive calculations. These errors are in fact *continuous errors*, approximated by evaluating the postprocessed piecewise polynomials on a fixed fine mesh and comparing with the exact values on the same mesh. In the Tables, we also give *discrete edge or cell errors* obtained by comparing the approximate edge or cell moments to the exact ones in 2-norm: because of the tranverse integration (which is implicit in the $k = 0$ case), we actually solve $1D$ coupled equations and the edge and cell moments are values at the edges or cell moments of for instance a function $u(x)$, which after transverse integration in the y direction is a transverse moment of order 0 or 1 of $u(x, y)$ as in Eq. (5.9). The underlying $1D$ approximation is in $\mathcal{P}_{k+2}$ but the symmetrical Radau rule in the direction considered is only exact for $\mathcal{P}_{2k+1}$ and therefore introduces numerical quadrature errors which have to be taken into account.

In Table I, we give the numerical results using MCk0 for the case A1. The main result in this table is that the continuous convergence order is equal to 2, a quite natural result since the approximation u_h is at most in $\mathcal{P}_1$ and the poorest quadrature used to approximate the stiffness matrices integrates exactly any member of $\mathcal{Q}_1$. We have checked that the same is true for the next three cases, namely A2, A3, and A4. The discrete edge and cell convergence orders are also equal to 2, in spite of the fact that the underlying approximation is quadratic: this is due to the symmetrical Radau rule, which is only correct for $\mathcal{P}_1$.

Using MCk1, the numerical results for the case A1 are shown in Tables II and III. The continuous convergence order is 3 as predicted by the theory, since all the quadrature rules used are correct for $\mathcal{Q}_3$ and two edge moments only are conserved through the edges.

In Table II, one realizes that the convergence orders for the zeroth Legendre moments at edges are $O(h^4)$ while the first Legendre moments are only $O(h^3)$. Looking at Table III, it is found that 00 and 11 cell Legendre moments tend to $O(h^4)$ while moments 10 and 01 are $O(h^3)$. Similar results were found for

cases A2 to A4 using MCk1 and they are given (for the edge moments and the continuous error only) in Tables IV to VI.

A qualitative interpretation of the results obtained is as follows. The transverse moments of order $\ell = 0$ and 1 of $u(x, y)$ in the y direction are in fact approximated by cubic functions defined by their values at the left and right of each cell (m_L^ℓ and m_R^ℓ) as well as by two cell moments ($m_C^{0\ell}$ and $m_C^{1\ell}$). The numerical integration used in the horizontal direction is correct for $\mathcal{P}_3$, but no more. This prevents us from obtaining the usual superconvergences of $O(h^6)$ (resp. $O(h^5)$) for m_L^0, m_R^0, m_C^{00} (resp. m_C^{10}) explained for instance in Carey and Oden [6]. For the corresponding moments of order $\ell = 1$, the exponent of h decreases by one because of the presence of Δy_j at the denominator of $p_{j1}(y)$ in (5.7). With the numerical integration used, this becomes $O(h^4)$ for m_L^0, m_R^0, m_C^{00}, $O(h^3)$ for m_L^1, m_R^1, m_C^{10} and $O(h^2)$ for m_C^{11}. These theoretical predictions are well observed, except for m_C^{11} where unexpectedly the exponent two is replaced by four (or at least more than 3), a superconvergence result which is not explained at the time of this writing.

References

[1] Altiparmakov, D.V. and Tomašević (1990) Variational formulation of a higher order nodal diffusion method, *Nucl. Sci. Engng* **105**, 256–270.

[2] Arnold, D.N. and Brezzi, F. (1985) Mixed and nonconforming finite element methods: implementation, postprocessing and error estimates, *Mathematical Modelling and Numerical Analysis* **19**, 7–35.

[3] Babuška, I. and Kellogg, R.B. (1972) Numerical solution of the neutron diffusion equation in the presence of corners and interfaces, in *Numerical Reactor Calculations*, pp. 473–486, International Atomic Energy Agency, Vienna.

[4] Brezzi, F., Douglas, J., Jr., and Marini, L.D. (1985) Two families of mixed finite elements for second order elliptic problems, *Numer. Math.* **47**, 217–235.

[5] Brezzi, F., Douglas, J., Jr., Fortin, M. and Marini, L.D. (1987) Efficient rectangular mixed finite elements in two and three space variables, *Math. Mod. Numer. Anal.* **21**, 581–604.

[6] Carey, G.F. and Oden, J.T. (1983) *Finite Elements: A Second Course*, Prentice-Hall, Englewood Cliffs, New Jersey.

[7] Ciarlet, P.G. (1978) *The Finite Element Method for Elliptic Problems*, North Holland, Amsterdam.

[8] Ciarlet, P.G. (1991) Basic error estimates for elliptic problems, in *Handbook of Numerical Analysis, Vol II*, P.G. Ciarlet and J.L. Lions, Eds, pp. 19–351, North Holland, Amsterdam.

[9] Davis, P.J. and Rabinowitz, P. (1984) *Methods of Numerical Integration*, 2nd edition, Academic Press, Orlando, Florida.

[10] Ewing, R.E. and Shen, J. (1993) Convergence of a block finite difference scheme for second-order elliptic problems with discontinuous coefficients, Texas A&M University, Manuscript, 19 p..

[11] Ewing, R.E., Shen, J., and Wang, J. (1991) Application of superconvergence to problems in the simulation of miscible displacement, *Comp. Meth. Appl. Mech. Eng.* **89**, 73–84.

[12] Forsyth, P.A., Jr. and Sammon, P.H. (1988) Quadratic convergence for cell-centered grids *Applied Numerical Mathematics* **4**, 377–394.

[13] Hennart, J.P. (1986) A general family of nodal schemes, *SIAM J. Sci. Stat. Comput.* **7**, 264–287.

[14] Hennart, J.P. (1988) On the numerical analysis of analytical nodal methods, *Numer. Methods Partial Differen. Equ.* **4**, 233–254.

[15] Hennart, J.P. (1992) A finite element approach to point-and mesh-centered finite difference schemes over rectangular grids, *Ann. Nucl. Energy* **19**, 663–678.

[16] Hennart, J.P., Jaffré, J., and Roberts, J.E. (1988) A constructive method for deriving finite elements of nodal type, *Numer. Math.* **53**, 701–738.

[17] Hennart, J.P., Malambu, E., Mund, E.H., and del Valle, E. (1996) Efficient higher order nodal finite element formulations for neutron multigroup diffusion equations, *Nucl. Sci. Engng*, To Appear in the September Issue.

[18] Hennart, J.P. and Mund, E.H. (1977) Singularities in the finite element approximation of two-dimensional diffusion problems, *Nucl. Sci. Eng.* **62**, 55–68.

[19] Hennart, J.P. and del Valle, E. (1993) On the relationship between nodal schemes and mixed-hybrid finite elements, *Numerical Methods for Partial Differential Equations* **9**, 411–430.

[20] Lesaint, P. (1976) On the convergence of Wilson's nonconforming element for solving the elastic problem, *Comput. Methods Appl. Mech. Eng.* **7**, 1–16.

[21] Lawrence, R.D. (1986) Progress in nodal methods for the solution of the neutron diffusion and transport equations, *Prog. Nucl. Energy* **17**, 271–301.

[22] Manteuffel, T.A. and White, A.B., Jr. (1986) The numerical solution of second-order boundary value problems on nonuniform meshes, *Math. Comp.* **47**, 511–535.

[23] Nitsche, J.A. (1974) Convergence of nonconforming methods, in *Mathematical Aspects of Finite Elements in Partial Differential Equations*, C. de Boor, Ed., pp. 15–53, Academic Press, New York.

[24] Ougouag, A.M. and Rajic, H.L. (1988) A self-consistent higher order coarse-mesh nodal method, *Nucl. Sci. Engng* **100**, 332–341.

[25] Raviart, P.A. and Thomas, J.M. (1977) A mixed finite element method for second order elliptic problems, in *Mathematical Aspects of the Finite Element Method, Lecture Notes in Mathematics* **606**, 292–315, Springer, Berlin.

[26] Russell, T.F. and Wheeler, M.F. (1983) Finite element and finite difference methods for continuous flows in porous media, in *The Mathematics of Reservoir Simulation*, R.E. Ewing, Ed., pp. 35–106, SIAM, Philadelphia, Pa.

[27] Shen, J. (1996) A block finite difference scheme for second-order elliptic problems with discontinuous coefficients, *SIAM J. Numer. Anal.* **33**, 686–706.

[28] Strang, G. and Fix, G.J (1973) *An Analysis of the Finite Element Method*, Prentice-Hall, Englewood Cliffs. New Jersey.

[29] Weiser, A. and Wheeler, M.F. (1988) On convergence of block-centered finite difference for elliptic problems, *SIAM J. Numer. Anal.* **25**, 351–375.

Table I. Discrete and continuous errors and convergence orders for case A1 using MCk0

Mesh	ϵ_H^0, ϵ_V^0	α_H^0, α_V^0	ϵ_C^{00}	α_C^{00}	ϵ	α
2×2	3.510×10^{-1}	—–	7.680×10^{-1}	—–	8.702×10^{-1}	—–
4×4	1.366×10^{-1}	1.361	2.554×10^{-1}	1.588	2.782×10^{-1}	1.645
8×8	4.266×10^{-2}	1.680	7.165×10^{-2}	1.834	7.772×10^{-2}	1.840
16×16	1.155×10^{-2}	1.885	1.855×10^{-2}	1.950	2.003×10^{-2}	1.956

Table II. Discrete edge and continuous errors and convergence orders for case A1 using MCk1

Mesh	ϵ_H^0, ϵ_V^0	α_H^0, α_V^0	ϵ_H^1, ϵ_V^1	α_H^1, α_V^1	ϵ	α
2×2	4.989×10^{-2}	—–	1.366×10^{-1}	—–	1.113×10^{-1}	—–
4×4	3.363×10^{-3}	3.891	2.725×10^{-2}	2.326	1.654×10^{-2}	2.751
6×6	6.709×10^{-4}	3.976	9.114×10^{-3}	2.701	4.995×10^{-3}	2.953
8×8	2.132×10^{-4}	3.985	4.063×10^{-3}	2.808	2.114×10^{-3}	2.989

Table III. Discrete cell errors and convergence orders for case A1 using MCk1

Mesh	ϵ_C^{00}	α_C^{00}	ϵ_C^{10}, ϵ_C^{01}	α_C^{10}, α_C^{01}	ϵ_C^{11}	α_C^{11}
2×2	4.955×10^{-2}	—–	7.949×10^{-2}	—–	1.257×10^{-1}	—–
4×4	5.198×10^{-3}	3.253	2.567×10^{-2}	1.631	2.486×10^{-2}	2.338
6×6	1.069×10^{-3}	3.901	8.913×10^{-3}	2.608	7.182×10^{-3}	3.063
8×8	3.415×10^{-4}	3.966	4.014×10^{-3}	2.773	2.739×10^{-3}	3.351

Table IV. Discrete edge and continuous errors and convergence orders for case A2 using MCk1

Mesh	ϵ_H^0, ϵ_V^0	α_H^0, α_V^0	ϵ_H^1, ϵ_V^1	α_H^1, α_V^1	ϵ	α
2×2	3.363×10^{-3}	—	2.725×10^{-2}	—	1.663×10^{-2}	—
4×4	2.132×10^{-4}	3.980	4.063×10^{-3}	2.745	2.158×10^{-3}	2.947
6×6	4.225×10^{-5}	3.992	1.268×10^{-3}	2.873	6.416×10^{-4}	2.992
8×8	1.339×10^{-5}	3.996	5.479×10^{-4}	2.915	2.712×10^{-4}	2.993

Table V. Discrete edge and continuous errors and convergence orders for case A3 using MCk1

Mesh	ϵ_H^0, ϵ_V^0	α_H^0, α_V^0	ϵ_H^1, ϵ_V^1	α_H^1, α_V^1	ϵ	α
2×2	6.883×10^{-2}	—	1.902×10^{-1}	—	1.365×10^{-1}	—
4×4	6.455×10^{-3}	3.415	4.803×10^{-2}	1.986	2.260×10^{-2}	2.595
6×6	1.308×10^{-3}	3.938	1.685×10^{-2}	2.584	7.025×10^{-3}	2.882
8×8	4.316×10^{-4}	3.853	7.652×10^{-3}	2.743	3.000×10^{-3}	2.958

Table VI. Discrete edge and continuous errors and convergence orders for case A4 using MCk1

Mesh	ϵ_H^0, ϵ_V^0	α_H^0, α_V^0	ϵ_H^1, ϵ_V^1	α_H^1, α_V^1	ϵ	α
2×2	1.821×10^{-2}	—	7.096×10^{-2}	—	5.231×10^{-2}	—
4×4	1.357×10^{-3}	3.747	1.249×10^{-2}	2.506	7.122×10^{-3}	2.876
6×6	2.739×10^{-4}	3.946	4.048×10^{-3}	2.779	2.142×10^{-3}	2.964
8×8	8.737×10^{-5}	3.972	1.779×10^{-3}	2.854	9.081×10^{-4}	2.981

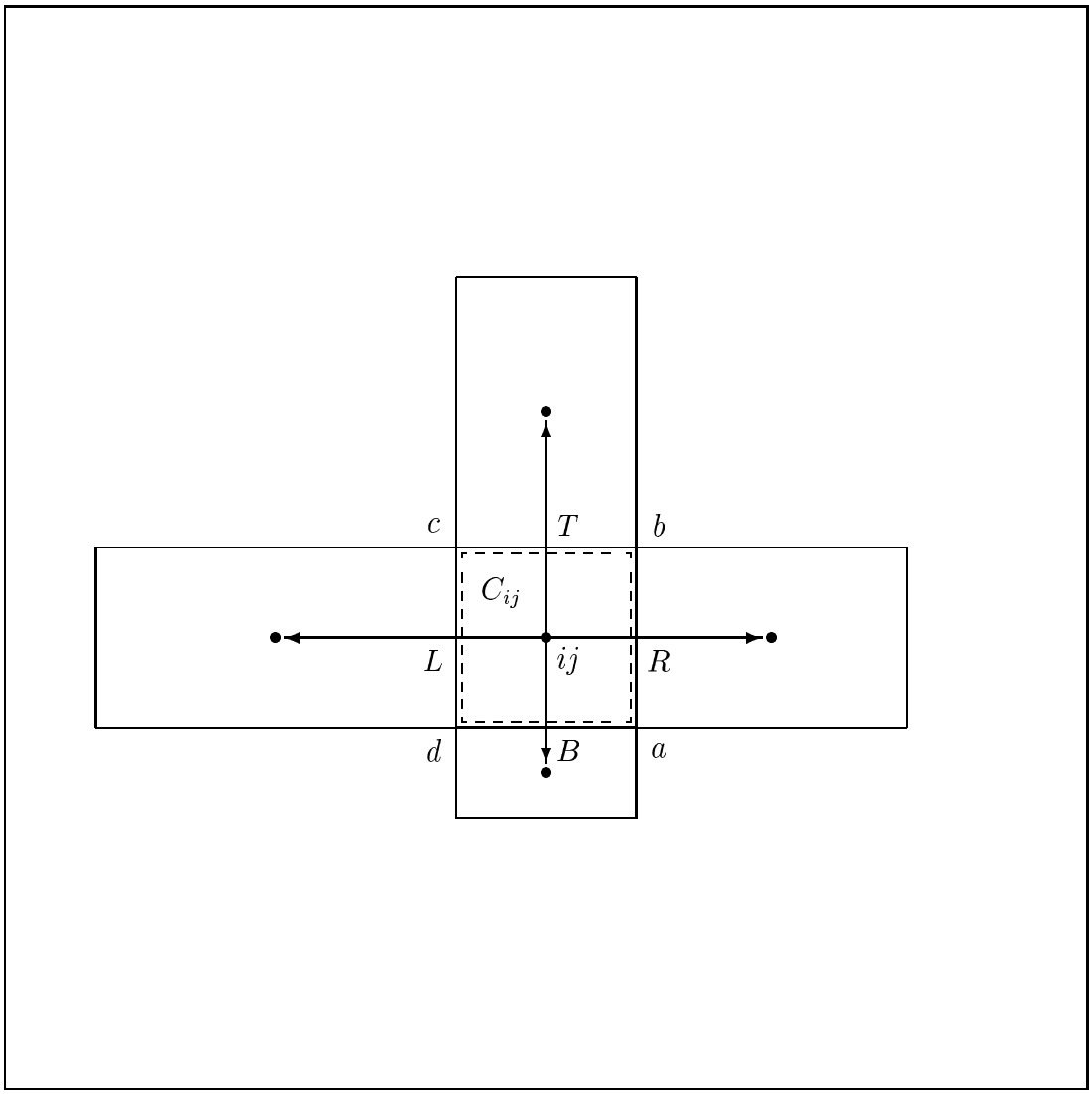

Figure 1. Reference cell C_{ij} and its closest neighbors.

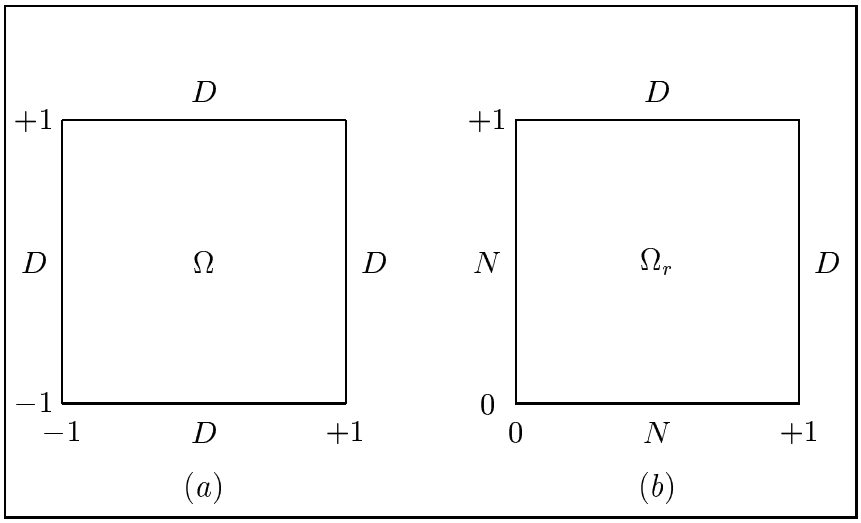

Figure 2. (a). The Domain Ω with Dirichlet Boundary Conditions
(b). The Domain Ω_r with Neumann and Dirichlet Boundary Conditions

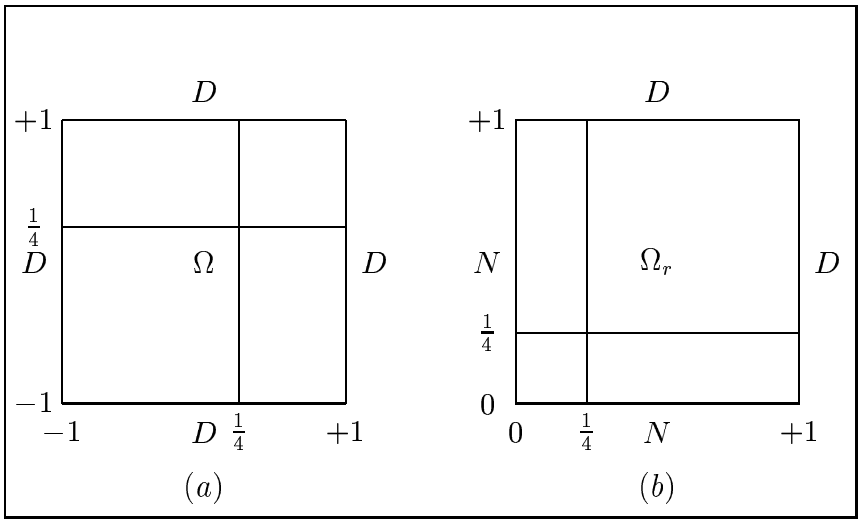

Figure 3. (a). The Domain Ω with starting grid and Dirichlet Boundary Conditions (b). The Domain Ω_r with starting grid and Neumann and Dirichlet Boundary Conditions

Unité de recherche INRIA Lorraine, Technopôle de Nancy-Brabois, Campus scientifique,
615 rue du Jardin Botanique, BP 101, 54600 VILLERS LÈS NANCY
Unité de recherche INRIA Rennes, Irisa, Campus universitaire de Beaulieu, 35042 RENNES Cedex
Unité de recherche INRIA Rhône-Alpes, 655, avenue de l'Europe, 38330 MONTBONNOT ST MARTIN
Unité de recherche INRIA Rocquencourt, Domaine de Voluceau, Rocquencourt, BP 105, 78153 LE CHESNAY Cedex
Unité de recherche INRIA Sophia-Antipolis, 2004 route des Lucioles, BP 93, 06902 SOPHIA-ANTIPOLIS Cedex

Éditeur
INRIA, Domaine de Voluceau, Rocquencourt, BP 105, 78153 LE CHESNAY Cedex (France)
ISSN 0249-6399

RR n ° 2979